Are bouncing scenarios a viable alternative to inflation?

L. Sriramkumar

Department of Physics, Indian Institute of Technology Madras, Chennai

Colloquium

Department of Physics, Indian Institute of Science, Bengaluru

August 30, 2019

Plan of the talk

1. Whither inflation?
2. Bouncing scenarios
3. Viable tensor-to-scalar ratio in a matter bounce scenario
4. Generating spectral tilt in near-matter bounces
5. Can bouncing scenarios lead to spectral features?
6. The tensor bispectrum in a matter bounce
7. Summary and outlook

This talk is based on. . .

- D. Chowdhury, V. Sreenath and L. Sriramkumar, *The tensor bispectrum in a matter bounce*, JCAP **1511**, 002 (2015) [arXiv:1506.06475 [astro-ph.CO]].
- R. N. Raveendran, D. Chowdhury and L. Sriramkumar, *Viable tensor-to-scalar ratio in a symmetric matter bounce*, JCAP **1801**, 030 (2018) [arXiv:1703.10061 [gr-qc]].
- R. N. Raveendran and L. Sriramkumar, *Viable scalar spectral tilt and tensor-to-scalar ratio in near-matter bounces*, arXiv:1812.06803 [astro-ph.CO].
- R. N. Raveendran and L. Sriramkumar, *Primordial features from ekpyrotic bounces*, Phys. Rev. D **99**, 043527 (2019) [arXiv:1809.03229 [astro-ph.CO]].

Plan of the talk

The horizon problem in the hot big bang model

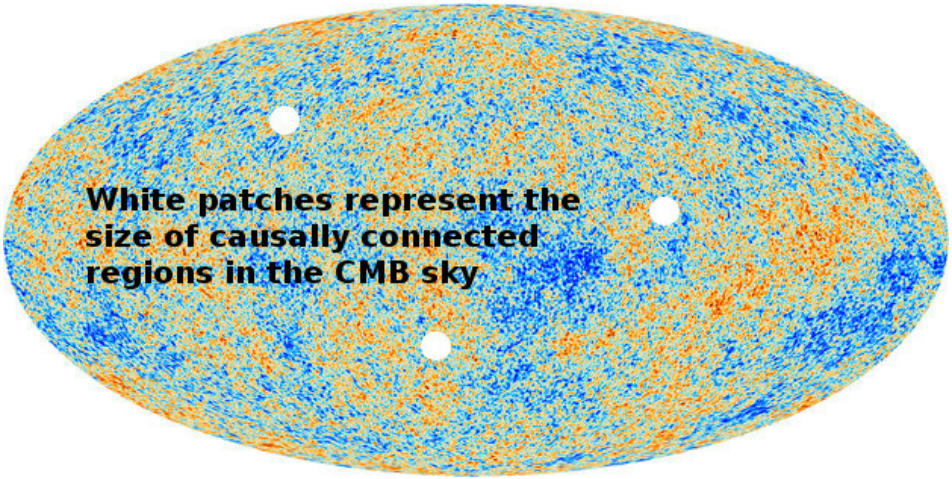

The radiation from the CMB arriving at us from regions separated by more than the Hubble radius at the last scattering surface, which subtends an angle of about 1° today, could not have interacted before decoupling.

The resolution of the horizon problem in inflation

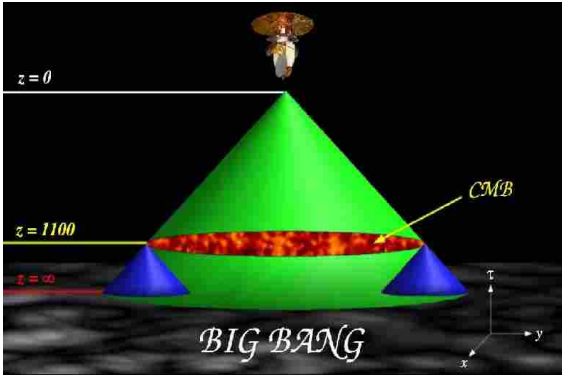

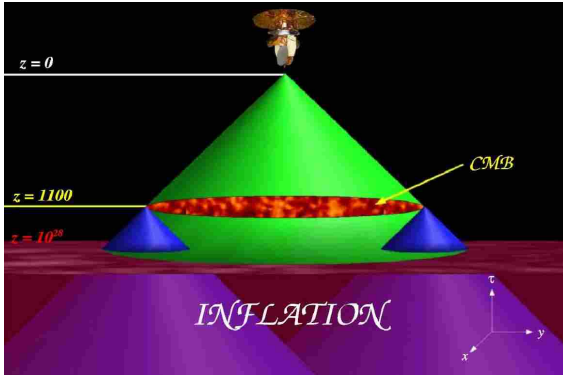

Another illustration of the horizon problem (on the left), and an illustration of its resolution (on the right) through an early and sufficiently long epoch of inflation[1].

Back to bounces

[1] Images from W. Kinney, astro-ph/0301448.

Bringing the modes inside the Hubble radius in inflation

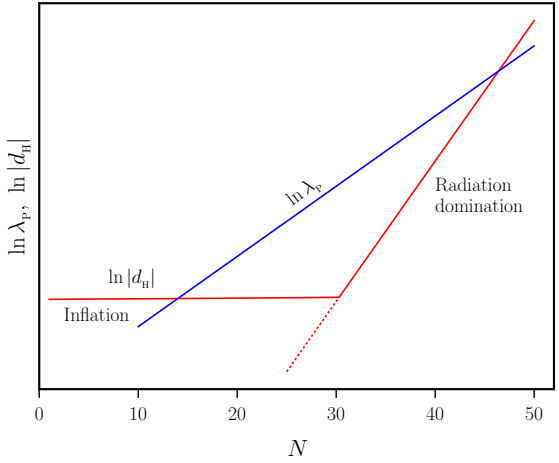

Back to bounces

The physical wavelength $\lambda_{\rm P} \propto a$ (in blue) and the Hubble radius $d_{\rm H} = H^{-1}$ (in red) in the inflationary scenario[2]. The scale factor is expressed in terms of e-folds N as $a(N) \propto {\rm e}^{N}$.

[2] See, for example, E. W. Kolb and M. S. Turner, *The Early Universe* (Addison-Wesley Publishing Company, New York, 1990), Fig. 8.4.

A variety of potentials to choose from

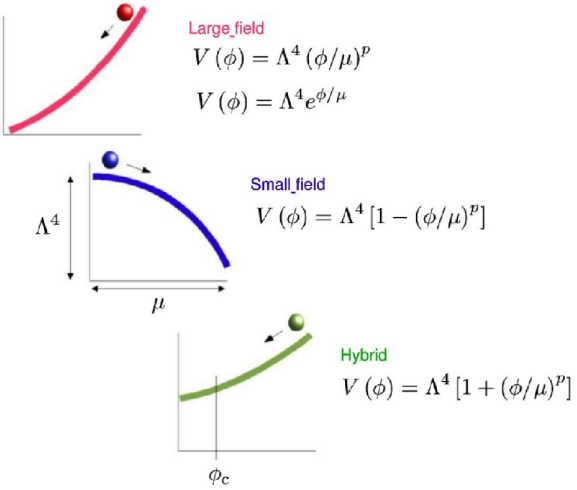

A variety of scalar field potentials have been considered to drive inflation[3]. Often, these potentials are classified as small field, large field and hybrid models.

[3] Image from W. Kinney, astro-ph/0301448.

Proliferation of inflationary models

5-dimensional assisted inflation
anisotropic brane inflation
anomaly-induced inflation
assisted inflation
assisted chaotic inflation
boundary inflation
brane inflation
brane-assisted inflation
brane gas inflation
brane-antibrane inflation
braneworld inflation
Brans-Dicke chaotic inflation
Brans-Dicke inflation
bulky brane inflation
chaotic hybrid inflation
chaotic inflation
chaotic new inflation
D-brane inflation
D-term inflation
dilaton-driven inflation
dilaton-driven brane inflation
double inflation
double D-term inflation
dual inflation
dynamical inflation
dynamical SUSY inflation
eternal inflation
extended inflation
extended open inflation
extended warm inflation
extra dimensional inflation
F-term inflation
F-term hybrid inflation
false vacuum inflation
false vacuum chaotic inflation
fast-roll inflation
first order inflation
gauged inflation
generalised inflation
generalized assisted inflation
generalized slow-roll inflation
gravity driven inflation
Hagedorn inflation
higher-curvature inflation
hybrid inflation
hyperextended inflation
induced gravity inflation
induced gravity open inflation
intermediate inflation
inverted hybrid inflation
isocurvature inflation
K inflation
kinetic inflation
lambda inflation
large field inflation
late D-term inflation
late-time mild inflation
low-scale inflation
low-scale supergravity inflation
M-theory inflation
mass inflation
massive chaotic inflation
moduli inflation
multi-scalar inflation
multiple inflation
multiple-field slow-roll inflation
multiple-stage inflation
natural inflation
natural Chaotic inflation
natural double inflation
natural supergravity inflation
new inflation
next-to-minimal supersymmetric hybrid inflation
non-commutative inflation
non-slow-roll inflation
nonminimal chaotic inflation
old inflation
open hybrid inflation
open inflation
oscillating inflation
polynomial chaotic inflation
polynomial hybrid inflation
power-law inflation
pre-Big-Bang inflation
primary inflation
primordial inflation
quasi-open inflation
quintessential inflation
R-invariant topological inflation
rapid asymmetric inflation
running inflation
scalar-tensor gravity inflation
scalar-tensor stochastic inflation
Seiberg-Witten inflation
single-bubble open inflation
spinodal inflation
stable starobinsky-type inflation
steady-state eternal inflation
steep inflation
stochastic inflation
string-forming open inflation
successful D-term inflation
supergravity inflation
supernatural inflation
superstring inflation
supersymmetric hybrid inflation
supersymmetric inflation
supersymmetric topological inflation
supersymmetric new inflation
synergistic warm inflation
TeV-scale hybrid inflation

A (partial?) list of ever-increasing number of inflationary models[4]. Actually, it may not even be possible to rule out some of these models!

[4] From E. P. S. Shellard, *The future of cosmology: Observational and computational prospects*, in *The Future of Theoretical Physics and Cosmology*, Eds. G. W. Gibbons, E. P. S. Shellard and S. J. Rankin (Cambridge University Press, Cambridge, England, 2003).

The quadratic action governing the perturbations

One can show that, at the quadratic order, the action governing the curvature perturbation $\mathcal{R}$ and the tensor perturbation γ_{ij} are given by[5]

$$\mathcal{S}_2[\mathcal{R}] = \frac{1}{2}\int \mathrm{d}\eta \int \mathrm{d}^3\boldsymbol{x}\; z^2 \left[\mathcal{R}'^2 - (\partial\mathcal{R})^2\right], \qquad \text{Back to the cubic scalar action}$$

$$\mathcal{S}_2[\gamma_{ij}] = \frac{M_{_{\rm Pl}}^2}{8}\int \mathrm{d}\eta \int \mathrm{d}^3\boldsymbol{x}\; a^2 \left[\gamma_{ij}'^2 - (\partial\gamma_{ij})^2\right]. \qquad \text{Back to the cubic tensor action}$$

These actions lead to the following equations of motion governing the scalar and tensor modes, say, f_k and h_k:

$$f_k'' + 2\,\frac{z'}{z}\,f_k' + k^2\,f_k = 0,$$

$$h_k'' + 2\,\frac{a'}{a}\,h_k' + k^2\,h_k = 0,$$

where $z = a\,M_{_{\rm Pl}}\sqrt{2\,\epsilon_1}$, with $\epsilon_1 = -\,\mathrm{d}\ln H/\mathrm{d}N$ being the first slow roll parameter.

[5] V. F. Mukhanov, H. A. Feldman and R. H. Brandenberger, Phys. Rep. **215**, 203 (1992).

From inside the Hubble radius to super-Hubble scales

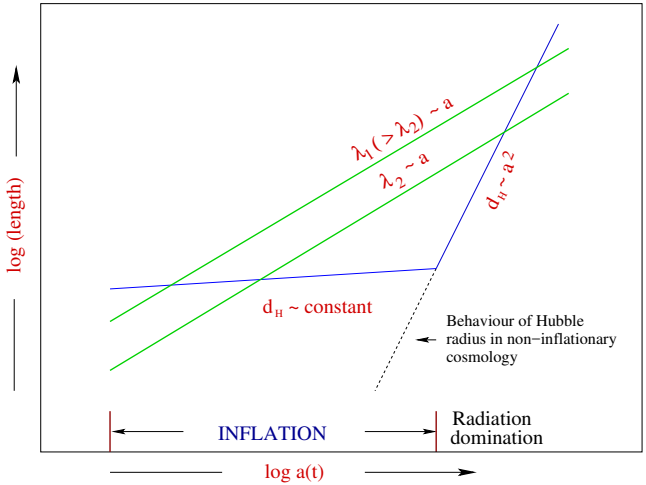

The initial conditions are imposed in the sub-Hubble regime when the modes are well inside the Hubble radius (*viz.* when $k/(a\,H) \gg 1$) and the power spectra are evaluated when they sufficiently outside (*i.e.* as $k/(a\,H) \ll 1$).

Typical evolution of the scalar modes

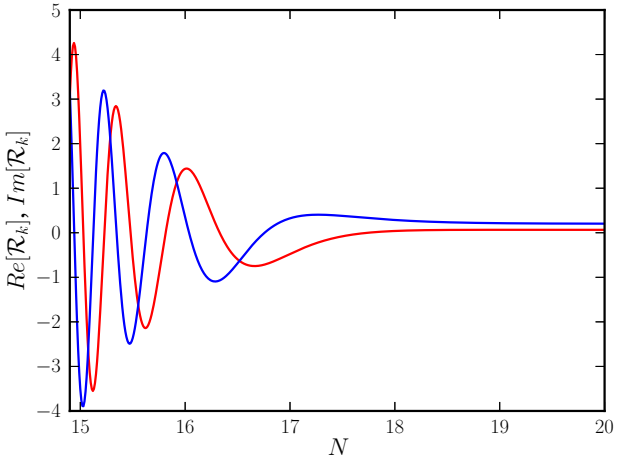

Typical evolution of the real and the imaginary parts of the scalar modes during slow roll inflation. The mode considered here leaves the Hubble radius at about 18 e-folds[6].

[6] Figure from V. Sreenath, *Computation and characteristics of inflationary three-point functions*, Ph.D. Thesis, Indian Institute of Technology Madras, Chennai, India (2015).

Spectral indices and the tensor-to-scalar ratio

While comparing with the observations, for convenience, one often uses the following power law, template scalar and the tensor spectra:

$$\mathcal{P}_{\rm S}(k) = \mathcal{A}_{\rm S}\left(\frac{k}{k_*}\right)^{n_{\rm S}-1}, \qquad \mathcal{P}_{\rm T}(k) = \mathcal{A}_{\rm T}\left(\frac{k}{k_*}\right)^{n_{\rm T}},$$

with the spectral indices $n_{\rm S}$ and $n_{\rm T}$ assumed to be constant.

The tensor-to-scalar ratio r is defined as

$$r(k) = \frac{\mathcal{P}_{\rm T}(k)}{\mathcal{P}_{\rm S}(k)}.$$

Performance of specific inflationary models in the $n_{\rm s}$-r plane

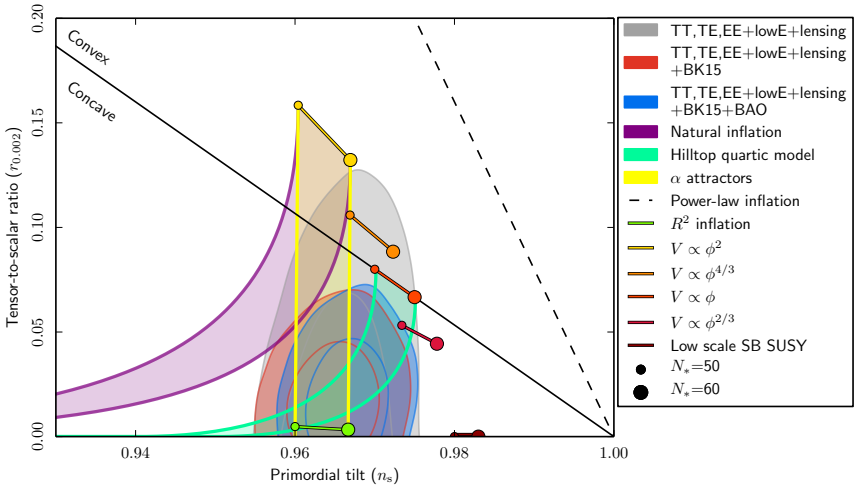

Joint constraints on $n_{\rm s}$ and $r_{0.002}$ from Planck in combination with other data sets, compared to the theoretical predictions of some of the popular inflationary models[7].

[7] Planck Collaboration (Y. Akrami *et al.*), arXiv:1807.06211 [astro-ph.CO].

Performance of inflationary models

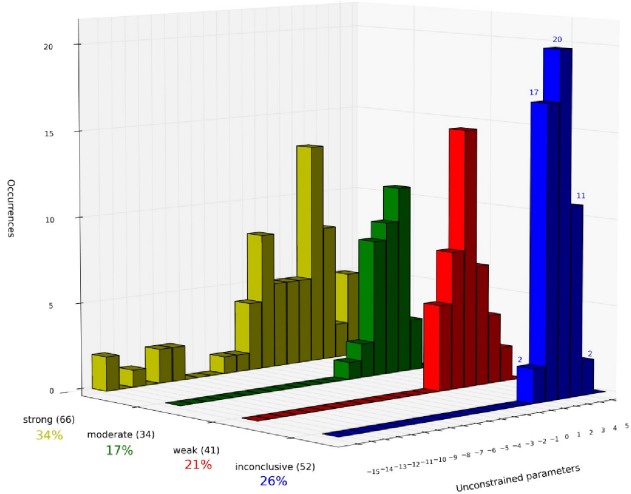

Proceed to bounces

The efficiency of the inflationary paradigm leads to a situation wherein, despite the strong constraints, a variety of models continue to remain consistent with the data[8].

[8] J. Martin, C. Ringeval, R. Trotta and V. Vennin, JCAP **1403**, 039 (2014).

The scalar bispectrum and the non-Gaussianity parameter $f_{\rm NL}$

The scalar bispectrum $\mathcal{B}_{\mathcal{R}\mathcal{R}\mathcal{R}}(\boldsymbol{k}_1, \boldsymbol{k}_2, \boldsymbol{k}_3)$ is related to the three point correlation function of the Fourier modes of the curvature perturbation, evaluated towards the end of inflation, say, at the conformal time $\eta_{\rm e}$, as follows[9]:

$$\langle \hat{\mathcal{R}}_{\boldsymbol{k}_1}(\eta_{\rm e})\, \hat{\mathcal{R}}_{\boldsymbol{k}_2}(\eta_{\rm e})\, \hat{\mathcal{R}}_{\boldsymbol{k}_3}(\eta_{\rm e}) \rangle = (2\,\pi)^3\ \mathcal{B}_{\mathcal{R}\mathcal{R}\mathcal{R}}(\boldsymbol{k}_1, \boldsymbol{k}_2, \boldsymbol{k}_3)\ \delta^{(3)}\left(\boldsymbol{k}_1 + \boldsymbol{k}_2 + \boldsymbol{k}_3\right).$$

The observationally relevant non-Gaussianity parameter $f_{\rm NL}$ is related to the scalar bispectrum through the following relation[10]:

$$\begin{aligned} f_{\rm NL}(\boldsymbol{k}_1, \boldsymbol{k}_2, \boldsymbol{k}_3) \ &= \ -\frac{10}{3}\,(2\,\pi)^{1/2}\ \left(k_1^3\, k_2^3\, k_3^3\right)\ \mathcal{B}_{\mathcal{R}\mathcal{R}\mathcal{R}}(\boldsymbol{k}_1, \boldsymbol{k}_2, \boldsymbol{k}_3) \\ &\quad \times\ \left[k_1^3\ \mathcal{P}_{\rm S}(k_2)\ \mathcal{P}_{\rm S}(k_3) + \text{two permutations}\right]^{-1}. \end{aligned}$$

[9] D. Larson *et al.*, Astrophys. J. Suppl. **192**, 16 (2011); E. Komatsu *et al.*, Astrophys. J. Suppl. **192**, 18 (2011).

[10] J. Martin and L. Sriramkumar, JCAP **1201**, 008 (2012).

The cubic order action governing the perturbations

It can be shown that, the third order term in the action describing the curvature perturbation is given by[11]

$$\mathcal{S}^3_{\mathcal{R}\mathcal{R}\mathcal{R}}[\mathcal{R}] = M_{_{\rm Pl}}^2 \int {\rm d}\eta \int {\rm d}^3\boldsymbol{x} \left[a^2\, \epsilon_1^2\, \mathcal{R}\, \mathcal{R}'^2 + a^2\, \epsilon_1^2\, \mathcal{R}\, (\partial\mathcal{R})^2 \right.$$
$$- 2\, a\, \epsilon_1\, \mathcal{R}'\, (\partial^i\mathcal{R})\, (\partial_i\chi) + \frac{a^2}{2}\, \epsilon_1\, \epsilon_2'\, \mathcal{R}^2\, \mathcal{R}' + \frac{\epsilon_1}{2}\, (\partial^i\mathcal{R})\, (\partial_i\chi)\, (\partial^2\chi)$$
$$\left. + \frac{\epsilon_1}{4}\, (\partial^2\mathcal{R})\, (\partial\chi)^2 + \mathcal{F}_1\left(\frac{\delta\mathcal{L}^2_{\mathcal{R}\mathcal{R}}}{\delta\mathcal{R}}\right) \right],$$

where $\mathcal{F}_1(\delta\mathcal{L}^2_{\mathcal{R}\mathcal{R}}/\delta\mathcal{R})$ denotes terms involving the variation of the second order action with respect to $\mathcal{R}$, while χ is related to the curvature perturbation $\mathcal{R}$ through the relation

$$\partial^2\chi = a\, \epsilon_1\, \mathcal{R}'.$$

▸ The quadratic action

[11] J. Maldacena, JHEP **0305**, 013 (2003);
D. Seery and J. E. Lidsey, JCAP **0506**, 003 (2005);
X. Chen, M.-x. Huang, S. Kachru and G. Shiu, JCAP **0701**, 002 (2007).

The shape of the slow roll bispectrum

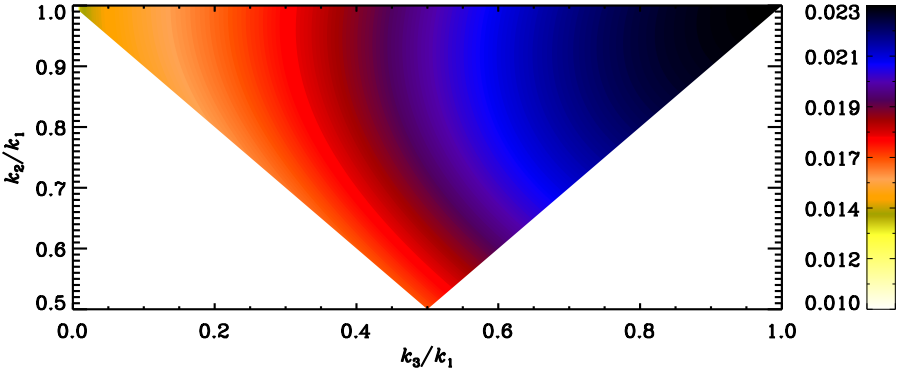

The non-Gaussianity parameter $f_{\rm NL}$ has been plotted as a function of k_3/k_1 and k_2/k_1 for the case of the popular quadratic potential. Note that the non-Gaussianity parameter peaks in the equilateral limit wherein $k_1 = k_2 = k_3$. In slow roll scenarios, the largest value of $f_{\rm NL}$ is found to be of the order of the first slow roll parameter ϵ_1[12].

[12] See, for example, D. Seery and J. E. Lidsey, JCAP **0506**, 003 (2005); X. Chen, Adv. Astron. **2010**, 638979 (2010).

Template bispectra

For comparison with the observations, the scalar bispectrum is often expressed in terms of the parameters $f_{\rm NL}^{\rm loc}$, $f_{\rm NL}^{\rm eq}$ and $f_{\rm NL}^{\rm orth}$ as follows:

$$G_{\mathcal{R}\mathcal{R}\mathcal{R}}(\boldsymbol{k}_1,\boldsymbol{k}_2,\boldsymbol{k}_3) = f_{\rm NL}^{\rm loc}\, G_{\mathcal{R}\mathcal{R}\mathcal{R}}^{\rm loc}(\boldsymbol{k}_1,\boldsymbol{k}_2,\boldsymbol{k}_3) + f_{\rm NL}^{\rm eq}\, G_{\mathcal{R}\mathcal{R}\mathcal{R}}^{\rm eq}(\boldsymbol{k}_1,\boldsymbol{k}_2,\boldsymbol{k}_3) + f_{\rm NL}^{\rm orth}\, G_{\mathcal{R}\mathcal{R}\mathcal{R}}^{\rm orth}(\boldsymbol{k}_1,\boldsymbol{k}_2,\boldsymbol{k}_3).$$

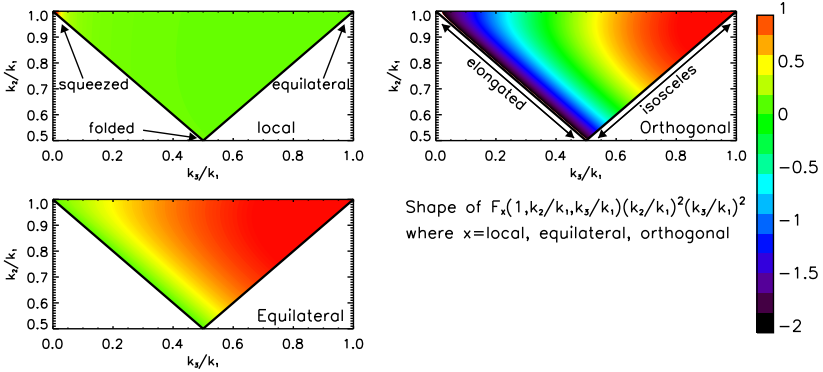

Illustration of the three template basis bispectra[13].

[13] E. Komatsu, Class. Quantum Grav. **27**, 124010 (2010).

Constraints on the scalar non-Gaussianity parameters

The constraints on the primordial values of the non-Gaussianity parameters from the Planck data are as follows[14]:

$$
\begin{aligned}
f_{\rm NL}^{\rm loc} &= -0.9 \pm 5.1, \\
f_{\rm NL}^{\rm eq} &= -26 \pm 47, \\
f_{\rm NL}^{\rm ortho} &= -38 \pm 24.
\end{aligned}
$$

These constraints imply that slowly rolling single field models involving the canonical scalar field which are favored by the data at the level of power spectra are also consistent with the data at the level of non-Gaussianities.

Back to outlook

[14] Planck Collaboration (Y. Akrami *et al.*), arXiv:1905.05697 [astro-ph.CO].

Plan of the talk

Bouncing scenarios as an alternative paradigm[15]

- Bouncing models correspond to situations wherein the universe initially goes through a period of contraction until the scale factor reaches a certain minimum value before transiting to the expanding phase.
- They offer an alternative to inflation to overcome the horizon problem, as they permit well motivated, Minkowski-like initial conditions to be imposed on the perturbations at early times during the contracting phase.
- However, matter fields *will* have to violate the null energy condition near the bounce in order to give rise to such a scale factor. Also, there exist (genuine) concerns whether such an assumption about the scale factor is valid in a domain where general relativity can be supposed to fail and quantum gravitational effects are expected to take over.

[15] See, for instance, M. Novello and S. P. Bergliaffa, Phys. Rep. **463**, 127 (2008); D. Battefeld and P. Peter, Phys. Rep. **571**, 1 (2015).

Bringing the modes inside the Hubble radius in bounces

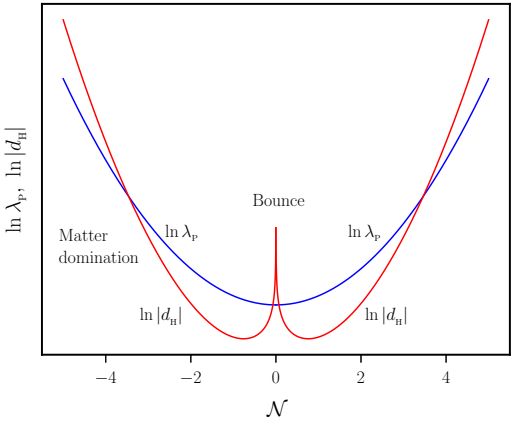

▸ Overcoming the horizon problem

▸ Behavior in inflation

The physical wavelength $\lambda_{\rm P} \propto a$ and the Hubble radius $d_{\rm H} = H^{-1}$ in a bouncing scenario[16]. The scale factor is expressed as $a(\mathcal{N}) \propto \mathrm{e}^{\mathcal{N}^2/2}$. For modes to be inside the Hubble radius at early times, the universe needs to undergo *non-accelerated contraction*.

[16] Figure from, D. Chowdhury, *Inflation, bounces and primordial correlations*, Ph.D. Thesis, Indian Institute of Technology Madras, Chennai, 2018.

Classical bounces and sources

Consider, for instance, bouncing models of the form

$$a(\eta) = a_0 \left(1 + \frac{\eta^2}{\eta_0^2}\right)^{1+\varepsilon} = a_0 \left(1 + k_0^2\,\eta^2\right)^{1+\varepsilon},$$

where a_0 is the value of the scale factor at the bounce (*i.e.* when $\eta = 0$), $\eta_0 = 1/k_0$ denotes the time scale of the duration of the bounce, and $\varepsilon > 0$.

The above scale factor can be achieved with the help of two fluids (with constant equation of state parameters) whose energy densities behave as

$$\rho_1 = \frac{\rho_0}{(a/a_0)^{(3+2\,\varepsilon)/(1+\varepsilon)}}, \quad \rho_2 = -\frac{\rho_0}{(a/a_0)^{2\,(2+\varepsilon)/(1+\varepsilon)}}.$$

where $\rho_0 = 12\,M_{_{\rm Pl}}^2\,(k_0/a_0)^2\,(1+\varepsilon)^2$.

Note that the model depends only on the parameters k_0/a_0 and ε. While $\varepsilon = 0$ corresponds to the matter bounce scenario, $\varepsilon \ll 1$ corresponds to near-matter bounces.

Behavior of $\dot{H}$ and ρ in a matter bounce

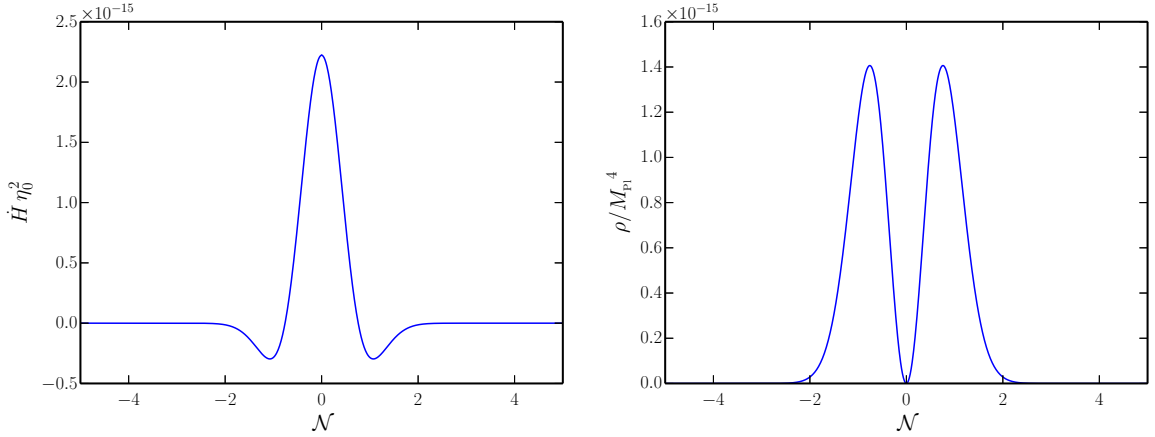

The behavior of $\dot{H} = -(\rho + p)/(2\,M_{\rm Pl}^2)$ (on the left) and the total energy density ρ (on the right) in the matter bounce scenario. Note that the null energy condition is violated near the bounce where $\dot{H} > 0$. The maximum value of ρ is much smaller than $M_{\rm Pl}^4$, which suggests that the bounce can be treated completely classically.

Back to scalar perturbations

Duality between de Sitter inflation and matter bounce

It is known that the solutions to the equations of motion governing the scalar and tensor perturbations are invariant under a certain transformation referred to as the duality transformation[17].

For instance, recall that the Mukhanov-Sasaki variable corresponding to the tensor perturbations [which is defined as $u_k = (M_{\rm Pl}/\sqrt{2})\, a\, h_k$] satisfies the differential equation

$$u_k'' + \left(k^2 - \frac{a''}{a}\right) u_k = 0.$$

Given a scale factor a, the corresponding dual, say, $\tilde{a}$, which leads to the same equation for the variable u_k is given by

$$a(\eta) \to \tilde{a}(\eta) = C\, a(\eta) \int_{\eta_*}^{\eta} \frac{{\rm d}\bar{\eta}}{a^2(\bar{\eta})},$$

where C and η_* are constants.

It is straightforward to show that the dual solution to de Sitter inflation corresponds to the matter bounce. Both these cases lead to scale invariant spectra.

[17] D. Wands, Phys. Rev. D **60**, 023507 (1999).

Plan of the talk

The matter bounce

We shall assume that the scale factor describing the bouncing scenario is given in terms of the conformal time coordinate η by the relation

$$a(\eta) = a_0 \left(1 + \eta^2/\eta_0^2\right) = a_0 \left(1 + k_0^2\,\eta^2\right).$$

As we had discussed earlier, at very early times, *viz.* when $\eta \ll -\eta_0$, the scale factor behaves as in a matter dominated epoch[18].

The quantity a''/a corresponding to the above scale factor is given by

$$\frac{a''}{a} = \frac{2\,k_0^2}{1 + k_0^2\,\eta^2},$$

which is essentially a Lorentzian profile.

[18] See, for example, R. Brandenberger, arXiv:1206.4196.

The behavior of a''/a

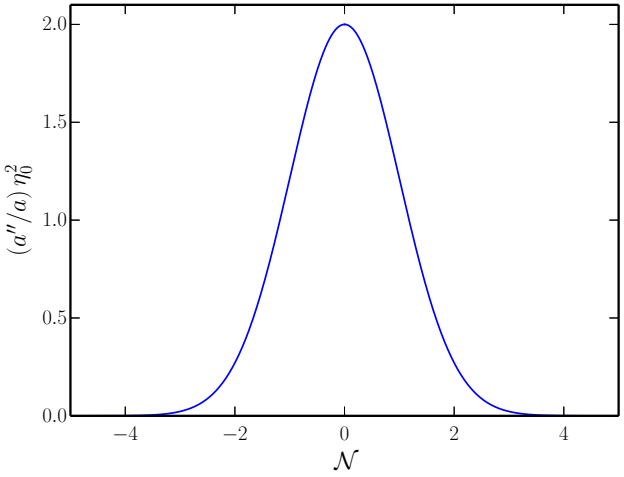

The behavior of the quantity a''/a in the matter bounce scenario of interest. Note that the maximum value of a''/a is of the order of k_0^2.

▸ Evolution of h_k, sans the details

The tensor modes in the first domain

We are interested in the evolution of the modes until some time after the bounce which corresponds to, say, the epoch of reheating in the conventional big bang model.

Let us divide this period into two domains, with the first domain determined by the condition $-\infty < \eta < -\alpha\,\eta_0$, where α is a relatively large number, which we shall set to be, say, 10^5.

In the first domain, we can assume that the scale factor behaves as $a(\eta) \simeq a_0\,k_0^2\,\eta^2$, so that $a''/a \simeq 2/\eta^2$. Since the condition $k^2 = a''/a$ corresponds to, say, $\eta_k = -\sqrt{2}/k$, the initial conditions can be imposed when $\eta \ll \eta_k$.

The modes h_k can be easily obtained in such a case and the positive frequency modes that correspond to the vacuum state at early times are given by

$$h_k(\eta) = \frac{\sqrt{2}}{M_{_{\rm Pl}}}\,\frac{1}{\sqrt{2\,k}}\,\frac{1}{a_0\,k_0^2\,\eta^2}\,\left(1 - \frac{i}{k\,\eta}\right)\,{\rm e}^{-i\,k\,\eta}.$$

The modes in the second domain

Let us now consider the behavior of the modes in the domain $-\alpha\,\eta_0 < \eta < \beta\,\eta_0$, where, say, $\beta \simeq 10^2$. Since we are interested in scales much smaller than k_0, we shall assume that $\eta_k \ll -\alpha\,\eta_0$, which corresponds to $k \ll k_0/\alpha$.

In such a case, upon ignoring the k^2 term, the equation governing h_k can be immediately integrated to yield

$$h_k(\eta) \simeq h_k(\eta_*) + h_k'(\eta_*)\,a^2(\eta_*)\int_{\eta_*}^{\eta}\frac{\mathrm{d}\tilde{\eta}}{a^2(\tilde{\eta})},$$

where η_* is a suitably chosen time and the scale factor $a(\eta)$ is given by the complete expression.

If we choose $\eta_* = -\alpha\,\eta_0$, we can make use of the solution in the first domain to determine the constants and express the solution in the second domain as follows:

$$h_k = \mathcal{A}_k + \mathcal{B}_k\,f(k_0\,\eta),$$

where the function $f(k_0\,\eta)$ is given by

Back to scalar perturbations

$$f(k_0\,\eta) = \frac{k_0\,\eta}{1 + k_0^2\,\eta^2} + \tan^{-1}(k_0\,\eta)\,.$$

Evolution of the tensor modes across the bounce

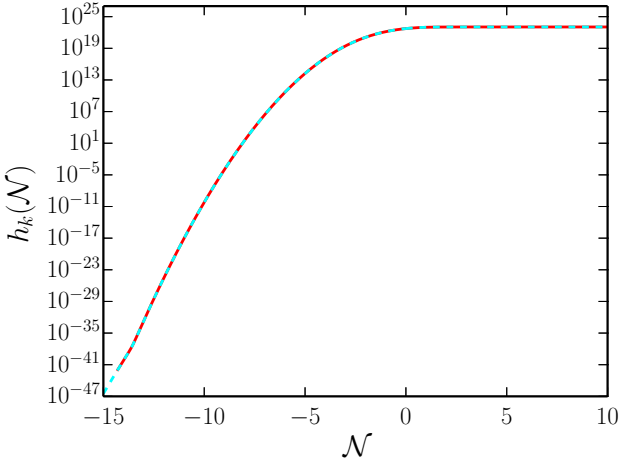

▸ Tensor power spectrum, sans the details

The numerical (in solid red) and the analytical results (in dashed cyan) for the amplitude of the tensor mode $|h_k|$ corresponding to $k/k_0 = 10^{-20}$. We have set $k_0/(a_0\, M_{\rm Pl}) = 3.3\times10^{-8}$ and have chosen $\alpha = 10^5$ for plotting the analytical results[19].

[19] D. Chowdhury, V. Sreenath and L. Sriramkumar, JCAP **1511**, 002 (2015).

The tensor power spectrum after the bounce

The quantities $\mathcal{A}_k$ and $\mathcal{B}_k$ are given by

$$\mathcal{A}_k = \frac{\sqrt{2}}{M_{_{\rm Pl}}}\,\frac{1}{\sqrt{2\,k}}\,\frac{1}{a_0\,\alpha^2}\,\left(1+\frac{i\,k_0}{\alpha\,k}\right)\,{\rm e}^{i\,\alpha\,k/k_0} + \mathcal{B}_k\,f(\alpha),$$

$$\mathcal{B}_k = \frac{\sqrt{2}}{M_{_{\rm Pl}}}\,\frac{1}{\sqrt{2\,k}}\,\frac{1}{2\,a_0\,\alpha^2}\,\left(1+\alpha^2\right)^2\,\left(\frac{3\,i\,k_0}{\alpha^2\,k}+\frac{3}{\alpha}-\frac{i\,k}{k_0}\right)\,{\rm e}^{i\,\alpha\,k/k_0}.$$

If we evaluate the tensor power spectrum after the bounce at $\eta = \beta\,\eta_0$, we find that it can be expressed as

$$\mathcal{P}_{_{\rm T}}(k) = 4\,\frac{k^3}{2\,\pi^2}\,|\mathcal{A}_k + \mathcal{B}_k\,f(\beta)|^2.$$

The tensor power spectrum

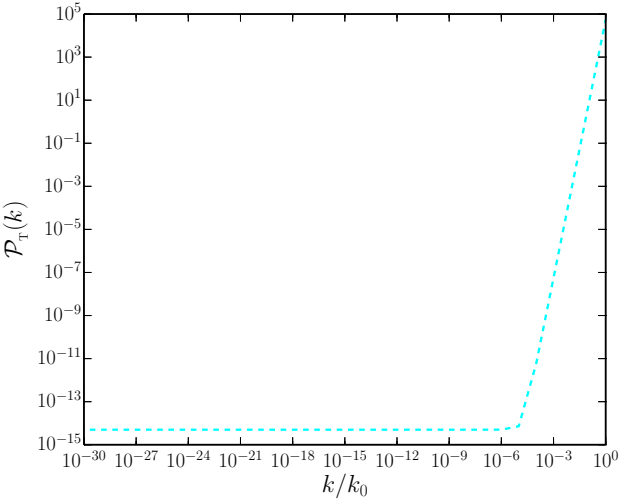

The tensor power spectrum, arrived at analytically, has been plotted as a function of k/k_0 for a wide range of wavenumbers. We have set $k_0/(a_0\, M_{\mathrm{P}l}) = 3.3 \times 10^{-8}$, $\alpha = 10^5$ and $\beta = 10^2$. Note that the power spectrum is scale invariant for $k \ll k_0/\alpha$.

A new model for the completely symmetric matter bounce

As we had discussed, the matter bounce scenario described by the scale factor

$$a(\eta) = a_0 \left(1 + \eta^2/\eta_0^2\right) = a_0 \left(1 + k_0^2\, \eta^2\right)$$

can be driven with the aid of two fluids, one which is matter and another fluid which behaves like radiation, but has negative energy density.

We find that the behavior can also be achieved with the help of two scalar fields, say, ϕ and χ, that are governed by the following action[20]:

$$S[\phi, \chi] = -\int \mathrm{d}^4x\, \sqrt{-g}\, \left[\frac{1}{2}\, \partial_\mu\phi\, \partial^\mu\phi + V(\phi) + U_0\, \left(-\frac{1}{2}\, \partial_\mu\chi\, \partial^\mu\chi\right)^2\right],$$

where U_0 is a constant and the potential $V(\phi)$ is given by

$$V(\phi) = 6\, M_{_{\rm Pl}}^2\, \frac{k_0^2}{a_0^2}\, \cosh^{-6}\left(\frac{\phi - \phi_0}{\sqrt{12}\, M_{_{\rm Pl}}}\right).$$

[20] R. N. Raveendran, D. Chowdhury and L. Sriramkumar, JCAP **1801**, 030 (2018).

The scalar perturbations

When the scalar perturbations are taken into account, the FLRW line element can be written as

$$\mathrm{d}s^2 = -(1+2\,A)\,\mathrm{d}t^2 + 2\,a(t)\,(\partial_i B)\,\mathrm{d}t\,\mathrm{d}x^i + a^2(t)\,\left[(1-2\,\psi)\,\delta_{ij} + 2\,(\partial_i\,\partial_j E)\right]\,\mathrm{d}x^i\,\mathrm{d}x^j,$$

where, evidently, the quantities A, ψ, B and E represent the metric perturbations.

The gauge invariant curvature and isocurvature perturbations $\mathcal{R}$ and $\mathcal{S}$ can be defined in terms of the above metric perturbations and the perturbations $\delta\phi$ and $\delta\chi$ in the scalar fields as follows[21]:

$$\mathcal{R} = \frac{H}{\dot{\phi}^2 - U_0\,\dot{\chi}^4}\,\left(\dot{\phi}\,\overline{\delta\phi} - U_0\,\dot{\chi}^3\,\overline{\delta\chi}\right), \quad \mathcal{S} = \frac{H\,\sqrt{\alpha\,\dot{\chi}^2}}{\dot{\phi}^2 - U_0\,\dot{\chi}^4}\,\left(\dot{\chi}\,\overline{\delta\phi} - \dot{\phi}\,\overline{\delta\chi}\right).$$

The quantities $\overline{\delta\phi}$ and $\overline{\delta\chi}$ denote the gauge invariant versions of the perturbations in the scalar fields, and are given by

$$\overline{\delta\phi} = \delta\phi + \frac{\dot{\phi}\,\psi}{H}, \qquad \overline{\delta\chi} = \delta\chi + \frac{\dot{\chi}\,\psi}{H}.$$

[21] R. N. Raveendran, D. Chowdhury and L. Sriramkumar, JCAP **1801**, 030 (2018).

Equations governing the curvature and isocurvature perturbations

We obtain the equations of motion describing the gauge invariant perturbations $\mathcal{R}_k$ and $\mathcal{S}_k$ in our model to be

$$
\begin{aligned}
\mathcal{R}_k'' &+ \frac{2\left(7+9\,k_0^2\,\eta^2-6\,k_0^4\,\eta^4\right)}{\eta\,\left(1-3\,k_0^2\,\eta^2\right)^2\,\left(1+k_0^2\,\eta^2\right)}\,\mathcal{R}_k' - \frac{k^2\,\left(5+9\,k_0^2\,\eta^2\right)}{3\,\left(1-3\,k_0^2\,\eta^2\right)}\,\mathcal{R}_k \\
&= \frac{4\,\left(5+12\,k_0^2\,\eta^2\right)}{\sqrt{3}\,\eta\,\left(1-3\,k_0^2\,\eta^2\right)\,\sqrt{1+k_0^2\,\eta^2}}\,\mathcal{S}_k' - \frac{4\,\left[5-22\,k_0^2\,\eta^2-24\,k_0^4\,\eta^4+k^2\,\eta^2\,\left(1+k_0^2\,\eta^2\right)^2\right]}{\sqrt{3}\,\eta^2\,\left(1+k_0^2\,\eta^2\right)^{3/2}\,\left(1-3\,k_0^2\,\eta^2\right)}\,\mathcal{S}_k, \\
\mathcal{S}_k'' &- \frac{2\left(9+7\,k_0^2\,\eta^2+6\,k_0^4\,\eta^4\right)}{\eta\,\left(1-3\,k_0^2\,\eta^2\right)\,\left(1+k_0^2\,\eta^2\right)}\,\mathcal{S}_k' \\
&- \frac{18-85\,k_0^2\,\eta^2-25\,k_0^4\,\eta^4-6\,k_0^6\,\eta^6+k^2\,\eta^2\,\left(3-k_0^2\,\eta^2\right)\,\left(1+k_0^2\,\eta^2\right)^2}{\eta^2\,\left(1-3\,k_0^2\,\eta^2\right)\,\left(1+k_0^2\,\eta^2\right)^2}\,\mathcal{S}_k \\
&= \frac{4\sqrt{3}\,\left(3-2\,k_0^2\,\eta^2\right)}{\eta\,\sqrt{1+k_0^2\,\eta^2}\,\left(1-3\,k_0^2\,\eta^2\right)}\,\mathcal{R}_k' + \frac{4\,k^2\,\sqrt{1+k_0^2\,\eta^2}}{\sqrt{3}\,\left(1-3\,k_0^2\,\eta^2\right)}\,\mathcal{R}_k.
\end{aligned}
$$

▸ Behavior of $\dot{H}$

However, some of the coefficients diverge when $\dot{H}$ and/or H vanish.

▸ Evolution of $\mathcal{R}_k$ and $\mathcal{S}_k$, sans the details

The uniform-χ gauge

The issue of diverging coefficients can be avoided by working in a gauge wherein $\delta\chi = 0$[22].

In this gauge, the equations of motion for the metric perturbations A_k and ψ_k can be obtained to be

$$A_k'' + 4\,\mathcal{H}\,A_k' + \left(\frac{k^2}{3} - \frac{20\,a_0^2\,k_0^2}{a^2}\right) A_k = -3\,\mathcal{H}\,\psi_k' + \frac{4\,k^2}{3}\,\psi_k,$$

$$\psi_k'' - 2\,\mathcal{H}\,\psi_k' + k^2\,\psi_k = 2\,\mathcal{H}\,A_k' - \frac{20\,a_0^2\,k_0^2}{a^2}\,A_k,$$

where $\mathcal{H} = a'/a$. These equations prove to be helpful in evolving the scalar perturbations across the bounce.

Also, in the uniform-χ gauge, the curvature and isocurvature perturbations simplify to be

$$\mathcal{R}_k = \psi_k + \frac{2\,H\,M_{_{\rm Pl}}^2}{\dot{\phi}^2 - U_0\,\dot{\chi}^4}\left(\dot{\psi}_k + H\,A_k\right), \quad \mathcal{S}_k = \frac{2\,H\,M_{_{\rm Pl}}^2\,\sqrt{U_0\,\dot{\chi}^4}}{\left(\dot{\phi}^2 - U_0\,\dot{\chi}^4\right)\,\dot{\phi}}\left(\dot{\psi}_k + H\,A_k\right).$$

[22] L. E. Allen and D. Wands, Phys. Rev. **70**, 063515 (2004).

Solutions for $\mathcal{R}_k$ and $\mathcal{S}_k$ in the first domain

As in the case of tensors, we shall be interested in evaluating the power spectrum after the bounce at $\eta = \beta\,\eta_0$. Also, to arrive at the analytical approximations, as earlier, we shall divide period of interest into two domains, *viz.* $-\infty < \eta < -\alpha\,\eta_0$ and $-\alpha\,\eta_0 < \eta < \beta\,\eta_0$.

In the first domain, we find that the solution to the curvature perturbation can be arrived at as in the case of tensors and is given by

$$\mathcal{R}_k(\eta) \simeq \frac{1}{\sqrt{6\,k}\,M_{_{\rm Pl}}\,a_0\,k_0^2\,\eta^2}\left(1 - \frac{i}{k\,\eta}\right)\mathrm{e}^{-i\,k\,\eta}.$$

Using this solution, it is straightforward to obtain the following solution for the isocurvature perturbation at early times:

$$\begin{aligned}\mathcal{S}_k(\eta) \;\simeq\; & \frac{1}{9\,\sqrt{2\,k^3}\,a_0\,k_0^3\,M_{_{\rm Pl}}\eta^4}\Bigg(-12\,i\,(1 + i\,k\,\eta)\,\mathrm{e}^{-i\,k\,\eta} + \frac{9}{3^{1/4}}\,k\,k_0\,\eta^2\,\mathrm{e}^{-i\,k\,\eta/\sqrt{3}} \\ & + 4\,k^2\,\eta^2\,\mathrm{e}^{-i\,k\,\eta/\sqrt{3}}\left\{\pi + i\,\mathrm{Ei}\left[\mathrm{e}^{-i\,(3-\sqrt{3})\,k\,\eta/3}\right]\right\}\Bigg).\end{aligned}$$

Solutions for ψ_k and A_k in the second domain

In the second domain, upon ignoring the k^2 dependent terms, one finds that the combination $A_k + \psi_k$ satisfies the same equation of motion as the tensor modes.

This feature helps us obtain the solutions for A_k and ψ_k, and they are given by

$$
\begin{aligned}
A_k(\eta) + \psi_k(\eta) &\simeq \frac{\mathcal{C}_k}{2\,a_0^2}\, f(k_0\,\eta) + \mathcal{D}_k,\\
A_k(\eta) &\simeq \frac{\mathcal{C}_k\, k_0\,\eta}{4\,a_0^2\,(1 + k_0^2\,\eta^2)} + \mathcal{E}_k\, \mathrm{e}^{-2\,\sqrt{5}\,\tan^{-1}(k_0\,\eta)} + \mathcal{F}_k\, \mathrm{e}^{2\,\sqrt{5}\,\tan^{-1}(k_0\,\eta)},
\end{aligned}
$$

where $f(k_0\,\eta)$ is the same function that we had encountered earlier in the case of tensors, and $\mathcal{C}_k$, $\mathcal{D}_k$, $\mathcal{E}_k$ and $\mathcal{F}_k$ are four constants of integration.

▸ Function $f(k_0\,\eta)$

The four constants, *viz.* $\mathcal{C}_k$, $\mathcal{D}_k$, $\mathcal{E}_k$ and $\mathcal{F}_k$, are determined by matching the above solutions with the solutions for $\mathcal{R}_k$ and $\mathcal{S}_k$ in the first domain at $\eta = -\alpha\,\eta_0$.

Evolution of $\mathcal{R}_k$, $\mathcal{S}_k$ and h_k

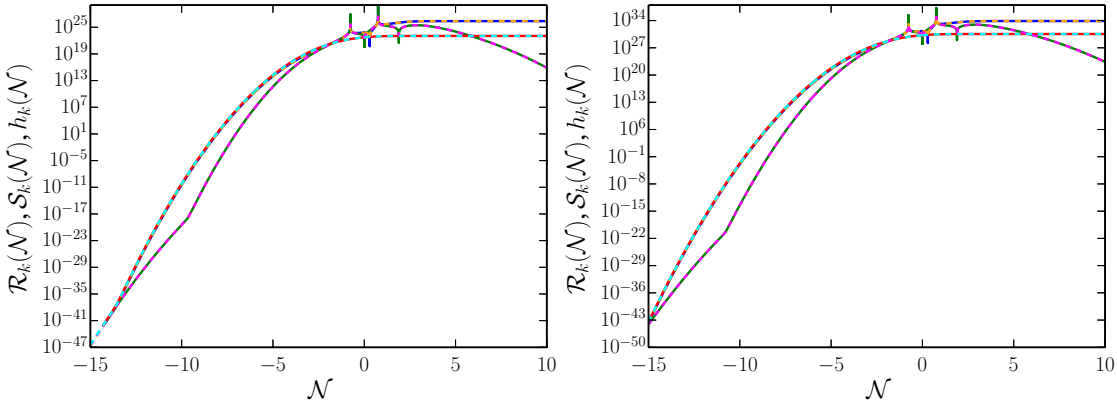

The evolution of the curvature, isocurvature and tensor perturbations, *viz.* $\mathcal{R}_k$ (in blue and orange), $\mathcal{S}_k$ (in green and magenta) and h_k (in red and cyan) across the bounce for the modes $k/k_0 = 10^{-20}$ (on the left) and $k/k_0 = 10^{-25}$ (on the right). We have set $k_0/(a_0\, M_{\rm Pl}) = 3.3 \times 10^{-8}$, $\alpha = 10^5$ and $\beta = 10^2$. The solid lines represent the results obtained numerically, while the dashed lines denote the analytical approximations.

The scalar and tensor power spectra in the matter bounce

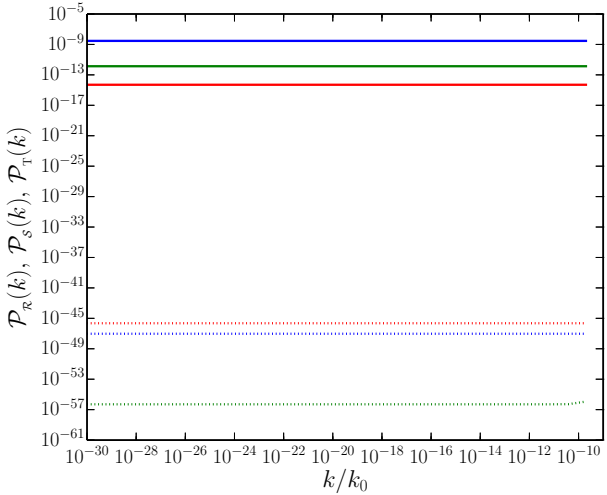

The scalar (curvature as blue and isocurvature as green) and tensor (as red) power spectra have been plotted before (as dotted lines) and after (as solid lines) the bounce[23].

[23] R. N. Raveendran, D. Chowdhury and L. Sriramkumar, JCAP **1801**, 030 (2018).

The evolution of the tensor-to-scalar ratio

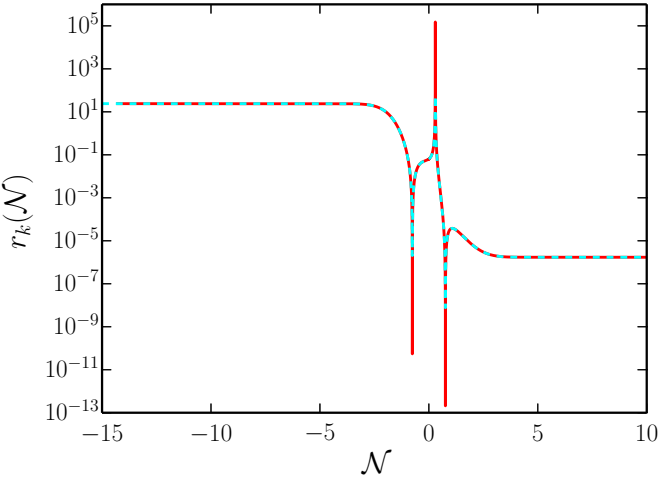

The evolution of the tensor-to-scalar ratio r across the matter bounce for a typical mode of cosmological interest. The solid (in red) and dashed (in cyan) lines represent the numerical and analytical results, respectively.

Plan of the talk

Driving near-matter bounces with scalar fields

Near-matter bounces can be described by the scale factor

$$a(\eta) = a_0 \left(1 + k_0^2\,\eta^2\right)^{(1+\varepsilon)}$$

with $\varepsilon \ll 1$, and one finds that a non-zero ε leads to a tilt in the power spectra.

Such a scale factor can also be achieved with the aid of two scalar fields, say, ϕ and χ, governed by the action[24]

$$S[\phi,\chi] = -\int \mathrm{d}^4x\,\sqrt{-g}\,\left[\frac{1}{2}\,\partial_\mu\phi\,\partial^\mu\phi + V(\phi) + U_0\,\left(-\frac{1}{2}\,\partial_\mu\chi\,\partial^\mu\chi\right)^{(2+\varepsilon)/(1+\varepsilon)}\right],$$

where U_0 is a constant of suitable dimensions, and the potential $V(\phi)$ is given by

$$V(\phi) = 2\,(3+4\,\varepsilon)\,(1+\varepsilon)\,M_{_{\rm Pl}}^2\,\frac{k_0^2}{a_0^2}\,\cosh^{-2\,(3+2\,\varepsilon)}\left(\frac{\phi-\phi_0}{\sqrt{4\,(1+\varepsilon)\,(3+2\,\varepsilon)}\,M_{_{\rm Pl}}}\right).$$

[24] R. N. Raveendran and L. Sriramkumar, arXiv:1812.06803 [astro-ph.CO].

Red-tilted scalar and tensor power spectra in a near-matter bounce

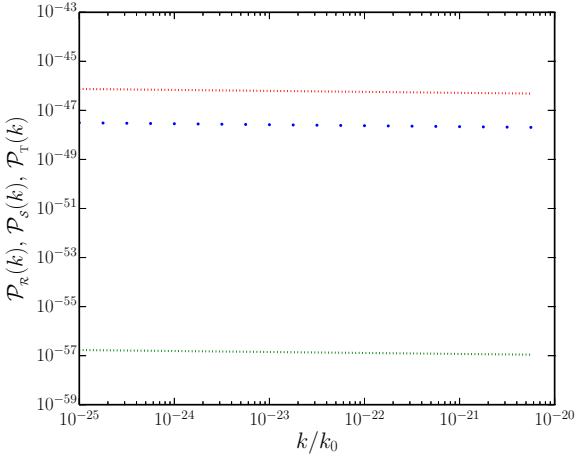

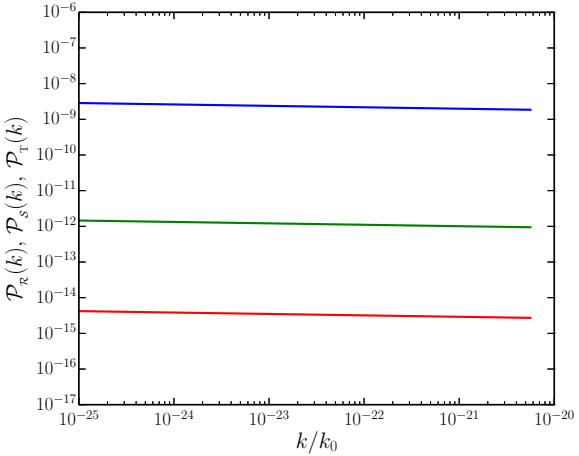

The scalar (curvature as blue and isocurvature as green) and tensor (as red) power spectra for $\varepsilon \simeq 10^{-2}$ (corresponding to a scalar spectral tilt of $n_{\mathrm{S}} = 0.96$) have been plotted before (as dotted lines, on the left) and after (as solid lines, on the right) the bounce[25].

[25] R. N. Raveendran, and L. Sriramkumar, arXiv:1812.06803 [astro-ph.CO].

Plan of the talk

CMB angular power spectrum from Planck: Are there outliers?

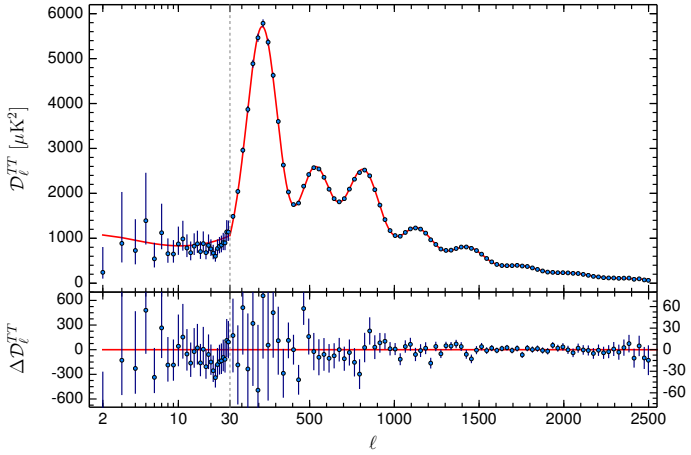

The CMB TT angular power spectrum from the Planck 2015 data (the blue dots with error bars) and the theoretical, best fit ΛCDM model with a power law primordial spectrum (the solid red curve)[26].

[26] Planck Collaboration (P. A. R. Ade *et al.*), Astron. Astrophys. **594**, A20 (2016).

Power spectra with features

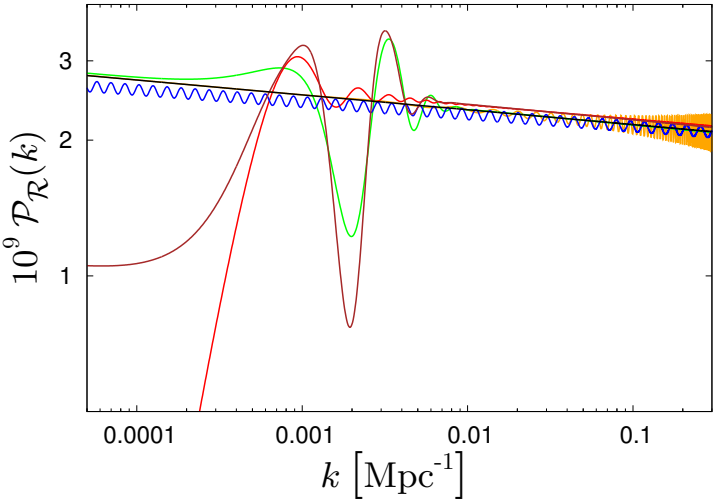

Primordial power spectra with features that lead to an improved fit to the data than the conventional, nearly scale, invariant spectra[27].

[27] Planck Collaboration (P. A. R. Ade *et al.*), Astron. Astrophys. **594**, A20 (2016).

Inflationary models permitting deviations from slow roll

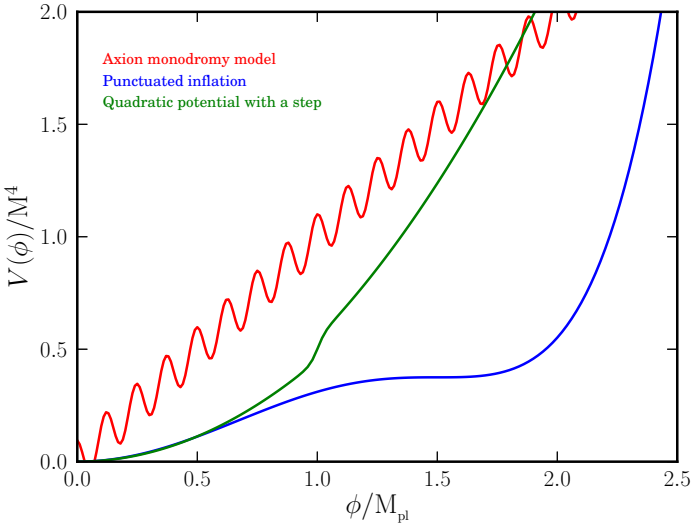

Illustration of potentials that admit departures from slow roll[28].

[28] D. K. Hazra, L. Sriramkumar and J. Martin, JCAP 1305, 026 (2013).

Spectra leading to an improved fit to the CMB data

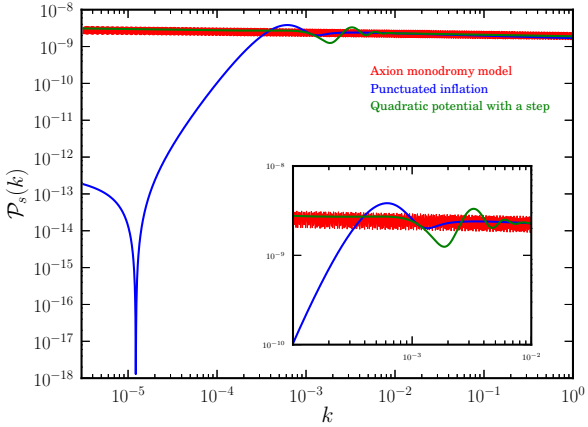

The scalar power spectra in different inflationary models that lead to a better fit to the CMB data than the conventional power law spectrum[29].

[29] R. K. Jain, P. Chingangbam, J.-O. Gong, L. Sriramkumar and T. Souradeep, JCAP **0901**, 009 (2009); D. K. Hazra, M. Aich, R. K. Jain, L. Sriramkumar and T. Souradeep, JCAP **1010**, 008 (2010); M. Aich, D. K. Hazra, L. Sriramkumar and T. Souradeep, Phys. Rev. D **87**, 083526 (2013).

Achieving stable contraction

The power law scale factor

$$a(\eta) = a_1 \left(\frac{\eta}{\eta_1}\right)^{2/(\lambda^2-2)}$$

corresponding to the constant equation of state $w = (\lambda^2 - 3)/3$, can be driven with the aid of a canonical scalar field described by the exponential potential

$$V(\phi) = V_0 \, \exp - \left(\frac{\lambda\,\phi}{M_{_{\rm Pl}}}\right) = -\frac{2}{(a_1\,\eta_1)^2}\,\frac{\lambda^2-6}{(\lambda^2-2)^2}\,\exp - \left(\frac{\lambda\,\phi}{M_{_{\rm Pl}}}\right).$$

It can be easily shown that, in an expanding universe, the solutions are stable when $\lambda^2 < 6$. Whereas, in a contracting universe, the solutions are found to be stable (*i.e.* they are attractors) when $\lambda^2 > 6$.

Note that, when $\lambda^2 > 6$, the potential $V(\phi)$ is *negative definite* resulting in $w > 1$. Such a *stiff* equation of state leads to a period of slow contraction (*i.e.* an ekpyrotic phase), which generates a *strongly blue* curvature perturbation spectrum[30].

[30] See, for instance, A. M. Levy, A. Ijjas and P. J. Steinhardt, Phys. Rev. D **92**, 063524 (2015).

Extending the single field model

The model we shall consider involves two scalar fields ϕ and χ, which are governed by the following action consisting of the potential $V(\phi, \chi)$ and a function $b(\phi)$[31]:

$$S[\phi, \chi] = \int \mathrm{d}^4x \, \sqrt{-g} \left[-\frac{1}{2} \, \partial_\mu \phi \, \partial^\mu \phi - \frac{\mathrm{e}^{2\, b(\phi)}}{2} \, \partial_\mu \chi \, \partial^\mu \chi - V(\phi, \chi) \right].$$

We shall work with the potential $V(\phi, \chi) = V_{\rm ek}(\phi) = V_0 \, \mathrm{e}^{-\lambda \, \phi / M_{\rm Pl}}$ and choose $b(\phi) = \mu \, \phi / (2 \, M_{\rm Pl})$, where λ and μ are positive constants.

To convert the isocurvature perturbations into curvature perturbations, since the field ϕ dominates during the ekpyrotic phase, we shall require a turn along the χ direction. We achieve such a turn by multiplying the original potential $V_{\rm ek}(\phi)$ by the term[32]

$$V_{\rm c}(\phi, \chi) = 1 + \beta \, \chi \exp - \left(\frac{\phi - \phi_{\rm c}}{\Delta \phi_{\rm c}} \right)^2,$$

where β, $\phi_{\rm c}$ and $\Delta \phi_{\rm c}$ are constants.

[31] See, for example, A. Ijjas, J.-L. Lehners and P. J. Steinhardt, Phys. Rev. D **89**, 123520 (2014).

[32] R. N. Raveendran and L. Sriramkumar, Phys. Rev. D **99**, 043527 (2019).

Converting isocurvature perturbations into curvature perturbations

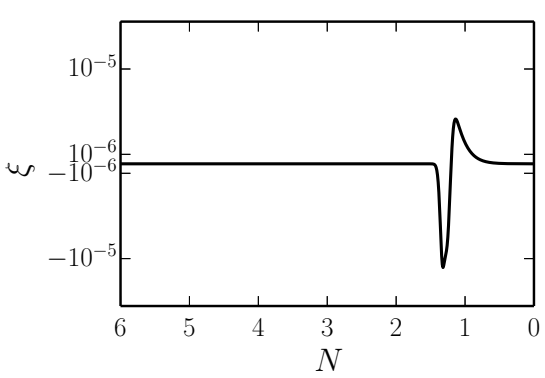

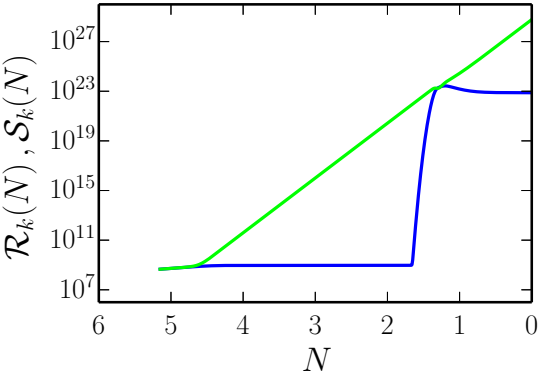

The behavior of the coupling function ξ (on the left) and the corresponding effects on the curvature (in blue) and the isocurvature (in green) perturbations (on the right) have been plotted as a function of e-folds N. Note that time runs forward from left to right and the choice of $N = 0$ is arbitrary[33].

[33] R. N. Raveendran and L. Sriramkumar, Phys. Rev. D **99**, 043527 (2019).

The effects of conversion on the power spectra

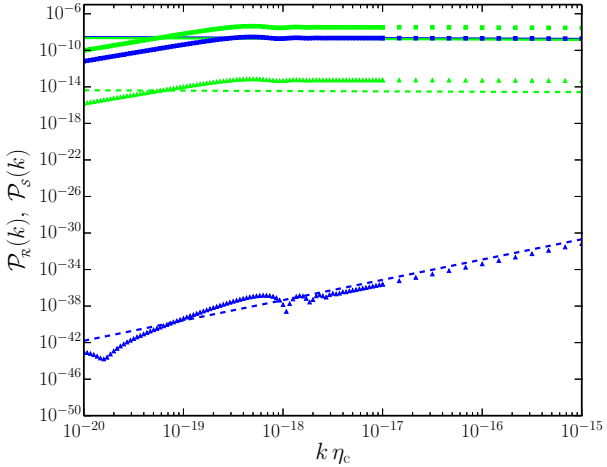

The spectra of the curvature and the isocurvature perturbations (in blue and green) have been plotted prior to (as dashed lines and triangles) as well as during the turn (as solid lines and squares) in field space[34].

[34] R. N. Raveendran and L. Sriramkumar, Phys. Rev. D **99**, 043527 (2019).

Features from ekpyrosis

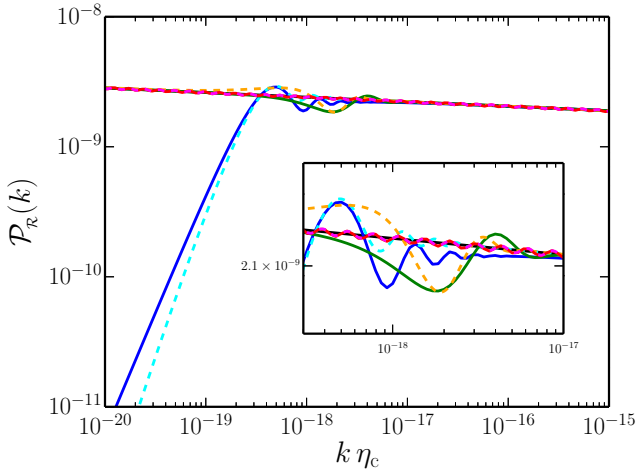

The power spectra of the curvature perturbation with the three types of features generated in the ekpyrotic (solid lines) and the inflationary (dashed lines) scenarios have been plotted over scales of cosmological interest[35].

▸ Proceed to summary and outlook

[35] R. N. Raveendran and L. Sriramkumar, Phys. Rev. D **99**, 043527 (2019).

Plan of the talk

Tensor bispectrum and non-Gaussianity parameter

The tensor bispectrum, evaluated at the conformal time, say, $\eta_{\rm e}$, is defined as

$$\langle \hat{\gamma}^{\boldsymbol{k}_1}_{m_1 n_1}(\eta_{\rm e})\, \hat{\gamma}^{\boldsymbol{k}_2}_{m_2 n_2}(\eta_{\rm e})\, \hat{\gamma}^{\boldsymbol{k}_3}_{m_3 n_3}(\eta_{\rm e})\rangle = (2\,\pi)^3\, \mathcal{B}^{m_1 n_1 m_2 n_2 m_3 n_3}_{\gamma\gamma\gamma}(\boldsymbol{k}_1, \boldsymbol{k}_2, \boldsymbol{k}_3) \times \delta^{(3)}\,(\boldsymbol{k}_1 + \boldsymbol{k}_2 + \boldsymbol{k}_3)$$

and, for convenience, we shall set

$$\mathcal{B}^{m_1 n_1 m_2 n_2 m_3 n_3}_{\gamma\gamma\gamma}(\boldsymbol{k}_1, \boldsymbol{k}_2, \boldsymbol{k}_3) = (2\,\pi)^{-9/2}\; G^{m_1 n_1 m_2 n_2 m_3 n_3}_{\gamma\gamma\gamma}(\boldsymbol{k}_1, \boldsymbol{k}_2, \boldsymbol{k}_3).$$

As in the scalar case, one can define a dimensionless non-Gaussianity parameter to characterize the amplitude of the tensor bispectrum as follows[36]:

$$h_{\rm NL}(\boldsymbol{k}_1, \boldsymbol{k}_2, \boldsymbol{k}_3) = -\left(\frac{4}{2\,\pi^2}\right)^2 \left[k_1^3\, k_2^3\, k_3^3\; G^{m_1 n_1 m_2 n_2 m_3 n_3}_{\gamma\gamma\gamma}(\boldsymbol{k}_1, \boldsymbol{k}_2, \boldsymbol{k}_3)\right] \times \left[\Pi^{\boldsymbol{k}_1}_{m_1 n_1, m_2 n_2}\, \Pi^{\boldsymbol{k}_2}_{m_3 n_3, \bar{m}\bar{n}}\; k_3^3\; \mathcal{P}_{\rm T}(k_1)\; \mathcal{P}_{\rm T}(k_2) + \text{five permutations}\right]^{-1}.$$

[36] V. Sreenath, R. Tibrewala and L. Sriramkumar, JCAP **1312**, 037 (2013).

The third order action and the tensor bispectrum

The third order action that leads to the tensor bispectrum is given by[37]

▸ The quadratic action

$$S^3_{\gamma\gamma\gamma}[\gamma_{ij}] = \frac{M_{\rm Pl}^2}{2}\int {\rm d}\eta \int {\rm d}^3\boldsymbol{x}\left[\frac{a^2}{2}\,\gamma_{lj}\,\gamma_{im}\,\partial_l\partial_m\gamma_{ij} - \frac{a^2}{4}\,\gamma_{ij}\,\gamma_{lm}\,\partial_l\partial_m\gamma_{ij}\right].$$

The tensor bispectrum calculated in the perturbative vacuum using the Maldacena formalism, can be written in terms of the modes h_k as follows:

$$\begin{aligned} G^{m_1n_1m_2n_2m_3n_3}_{\gamma\gamma\gamma}&(\boldsymbol{k}_1,\boldsymbol{k}_2,\boldsymbol{k}_3) \\ &= M_{\rm Pl}^2\left[\left(\Pi^{\boldsymbol{k}_1}_{m_1n_1,ij}\,\Pi^{\boldsymbol{k}_2}_{m_2n_2,im}\,\Pi^{\boldsymbol{k}_3}_{m_3n_3,lj} - \frac{1}{2}\,\Pi^{\boldsymbol{k}_1}_{m_1n_1,ij}\,\Pi^{\boldsymbol{k}_2}_{m_2n_2,ml}\,\Pi^{\boldsymbol{k}_3}_{m_3n_3,ij}\right)k_{1m}\,k_{1l}\right. \\ &\qquad \left. + \text{five permutations}\right] \\ &\qquad \times \left[h_{k_1}(\eta_{\rm e})\,h_{k_2}(\eta_{\rm e})\,h_{k_3}(\eta_{\rm e})\,\mathcal{G}_{\gamma\gamma\gamma}(\boldsymbol{k}_1,\boldsymbol{k}_2,\boldsymbol{k}_3) + \text{complex conjugate}\right], \end{aligned}$$

where $\mathcal{G}_{\gamma\gamma\gamma}(\boldsymbol{k}_1,\boldsymbol{k}_2,\boldsymbol{k}_3)$ is described by the integral

$$\mathcal{G}_{\gamma\gamma\gamma}(\boldsymbol{k}_1,\boldsymbol{k}_2,\boldsymbol{k}_3) = -\frac{i}{4}\int_{\eta_{\rm i}}^{\eta_{\rm e}} {\rm d}\eta\; a^2\,h^*_{k_1}\,h^*_{k_2}\,h^*_{k_3},$$

with $\eta_{\rm i}$ denoting the time when the initial conditions are imposed on the perturbations.

[37] J. Maldacena, JHEP **0305**, 013 (2003).

The contributions due to the three domains

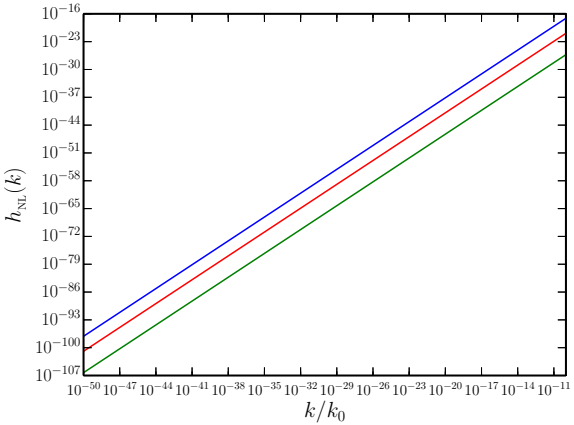

The contributions to the non-Gaussianity parameter $h_{\rm NL}$ in the equilateral limit from the first (in green), the second (in red) and the third (in blue) domains have been plotted as a function of k/k_0 for $k \ll k_0/\alpha$. Clearly, the third domain gives rise to the maximum contribution to $h_{\rm NL}$[38].

Skip the discussion on the squeezed limit

[38] D. Chowdhury, V. Sreenath and L. Sriramkumar, JCAP **1511**, 002 (2015).

The effect of the long wavelength tensor modes

Since the amplitude of a long wavelength mode freezes on super-Hubble scales during inflation, such modes can be treated as a background as far as the smaller wavelength modes are concerned. Let us denote the constant amplitude of the long wavelength tensor mode as $\gamma_{ij}^{\rm B}$.

In the presence of such a long wavelength mode, the background FLRW metric can be written as

$$\mathrm{d}s^2 = -\mathrm{d}t^2 + a^2(t)\,[\mathrm{e}^{\gamma^{\rm B}}]_{ij}\,\mathrm{d}\boldsymbol{x}^i\,\mathrm{d}\boldsymbol{x}^j,$$

i.e. the spatial coordinates are modified according to a spatial transformation of the form $\boldsymbol{x}' = \Lambda\,\boldsymbol{x}$, where $\Lambda_{ij} = [\mathrm{e}^{\gamma^{\rm B}/2}]_{ij}$.

Under such a spatial transformation, the small wavelength tensor perturbation transforms as[39]

$$\gamma_{ij}^{\boldsymbol{k}} \to \det\left(\Lambda^{-1}\right)\gamma_{ij}^{\Lambda^{-1}\,\boldsymbol{k}},$$

where $\det\left(\Lambda^{-1}\right) = 1$.

[39] S. Kundu, JCAP **1404**, 016 (2014).

The behavior of the two and three-point functions

On using the above results, one finds that the tensor two-point function in the presence of a long wavelength mode denoted by, say, the wavenumber k, can be written as

$$\langle \hat{\gamma}^{\boldsymbol{k}_1}_{m_1 n_1} \hat{\gamma}^{\boldsymbol{k}_2}_{m_2 n_2} \rangle_k = \frac{(2\,\pi)^2}{2\,k_1^3}\,\frac{\Pi^{\boldsymbol{k}_1}_{m_1 n_1, m_2 n_2}}{4}\,\mathcal{P}_{\rm T}(k_1)\,\delta^{(3)}(\boldsymbol{k}_1+\boldsymbol{k}_2) \times \left[1-\left(\frac{n_{\rm T}-3}{2}\right)\,\gamma^{\rm B}_{ij}\,\hat{n}_{1i}\,\hat{n}_{1j}\right],$$

where $\hat{n}_{1i} = k_{1i}/k_1$.

One can also show that, in the presence of a long wavelength mode, the tensor bispectrum can be written as[40]

$$\langle\, \hat{\gamma}^{\boldsymbol{k}_1}_{m_1 n_1}\, \hat{\gamma}^{\boldsymbol{k}_2}_{m_2 n_2}\, \hat{\gamma}^{\boldsymbol{k}_3}_{m_3 n_3}\, \rangle_{k_3} = -\frac{(2\,\pi)^{5/2}}{4\,k_1^3\,k_3^3}\left(\frac{n_{\rm T}-3}{32}\right)\,\mathcal{P}_{\rm T}(k_1)\,\mathcal{P}_{\rm T}(k_3) \times \Pi^{\boldsymbol{k}_1}_{m_1 n_1, m_2 n_2}\,\Pi^{\boldsymbol{k}_3}_{m_3 n_3, ij}\,\hat{n}_{1i}\,\hat{n}_{1j}\,\delta^3(\boldsymbol{k}_1+\boldsymbol{k}_2).$$

[40] V. Sreenath and L. Sriramkumar, JCAP **1410**, 021 (2014).

The complete contribution to $h_{\rm NL}$

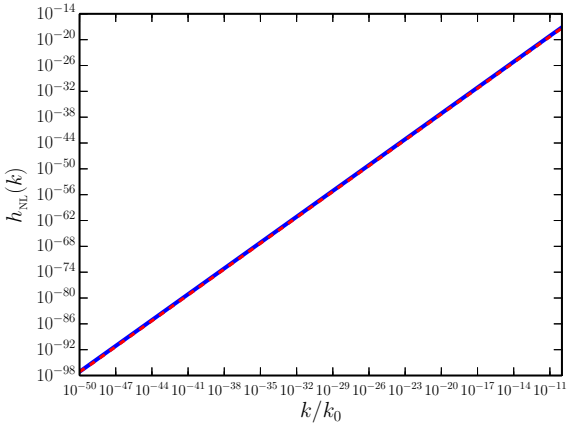

The behavior of $h_{\rm NL}$ in the equilateral (in blue) and the squeezed (in red) limits plotted as a function of k/k_0 for $k \ll k_0/\alpha$. The resulting $h_{\rm NL}$ is considerably small when compared to the values that arise in de Sitter inflation wherein $3/8 \lesssim h_{\rm NL} \lesssim 1/2$. Moreover, we find that $h_{\rm NL}$ behaves as k^2 in the equilateral and the squeezed limits, with similar amplitudes[41].

[41] D. Chowdhury, V. Sreenath and L. Sriramkumar, JCAP **1511**, 002 (2015).

Plan of the talk

Summary

- Earlier efforts had seemed to suggest that the tensor-to-scalar ratio may naturally be large in matter bounces.
- We have been able to construct a matter bounce scenario that leads to nearly scale invariant spectra and a tensor-to-scalar ratio that is consistent with the observations.
- Many of the simpler and fine tuned bouncing models would prove to be unsustainable if future observations confirm the presence of features. *For the first time*, we have constructed bouncing scenarios which lead to features that have often been found to provide an improved fit to the CMB data.
- Though we have evaluated the spectra prior to the bounce, since the scales associated with the bounce are expected to be significantly different from the scales of cosmological interest, the shape of the spectra we have arrived at are unlikely to be altered by the dynamics of the bounce[42].

[42] See, for example, A. Fertig, J.-L. Lehners, E. Mallwitz and E. Wilson-Ewing, JCAP **1610**, 005 (2016).

Outlook

- In inflation, classical perturbations present at early times will decay. In contrast, they can grow strongly during the contracting phase in bouncing models. So, such perturbations need to be assumed to be very small in smooth bounces.
- It has been argued that, due to the growth in the amplitude of the perturbations as one approaches the bounce, quite generically, the scalar non-Gaussianities generated in bounces may turn out to be large[43]. It has to be established that models which are consistent with the data at the level of power spectra also satisfy the current constraints on non-Gaussianities[44].

▸ Constraints on non-Gaussianities

- After the bounce, the universe needs to transit to a radiation dominated epoch. Such a transition has to be achieved, and the possible effects of the transition on the evolution of the large scale perturbations need to be examined[45].

[43] J. Quintin, Z. Sherkatghanad, Y-F. Cai and R. Brandenberger, Phys. Rev. D **92**, 062532 (2015); Y. B. Li, J. Quintin, D. G. Wang and Y. F. Cai, JCAP **1703**, 031 (2017).

[44] J.-L. Lehners, Adv. Astron. **2010**, 903907 (2010).

[45] Y-F. Cai, R. Brandenberger and X. Zhang, Phys. Letts. B **703**, 25 (2011).

Collaborators: former students

Rathul Nath Raveendran

Debika Chowdhury

V. Sreenath

Thank you for your attention